EUCALL

The European Cluster of Advanced Laser Light Sources

Grant Agreement number: 654220

Work package 7 – Work package PUCCA

Deliverable D7.1

Ultimate XGM sensitivities at FEL and ELI sources

Lead Beneficiary: DESY

Authors:
Stephan Klumpp and Kai Tiedtke

Due date: September 30th, 2016
Date of delivery: September 29th, 2016

Project webpage: www.eucall.eu

Deliverable Type	
R = Report DEM = Demonstrator, pilot, prototype, plan designs DEC = Websites, patents filing, press & media actions, videos, etc. OTHER = Software, technical diagram, etc.	R
Dissemination Level	
PU = Public, fully open, e.g. web CO = Confidential, restricted under conditions set out in Model Grant Agreement CI = Classified, information as referred to in Commission Decision 2001/844/EC	PU

This project has received funding from the *European Union's Horizon 2020 research and innovation programme* under grant agreement No 654220

Contents

This project has received funding from the *European Union's Horizon 2020 research and innovation programme* under grant agreement No 654220.

1 Properties of X-Ray Light Sources

In the late 19th century Wilhelm Conrad Röntgen discovered a so far unknown radiation which he named x-rays [1]. He examined the properties of the new radiation very carefully and determined it was able to penetrate objects which human eyesight could not. Famous became pictures of the bones of Röntgen's wife and of Albert von Kölliker (figure 1.1a). To see inside the human body without cutting it open marked a great step forward in medical diagnosis.

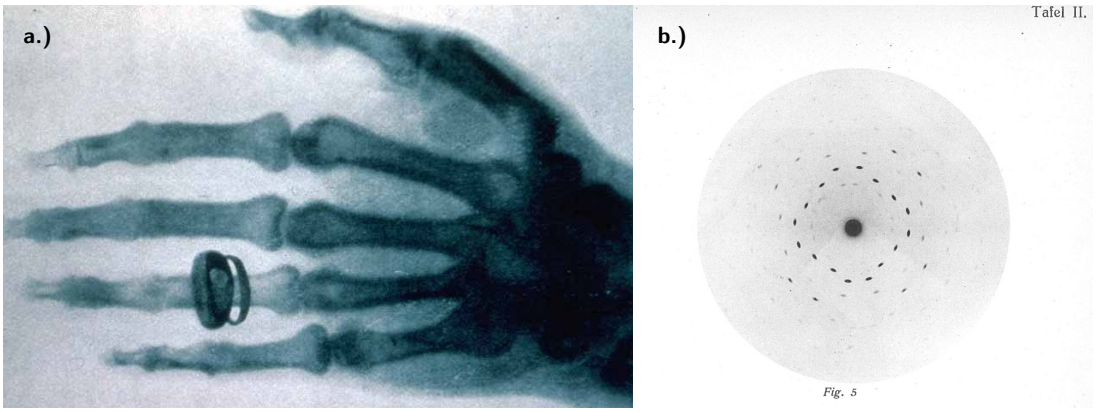

Figure 1.1: X-ray photograph of Albert von Kölliker's left hand taken at a public lecture of Röntgen in 1896. It was von Kölliker suggestion during the lecture to name x-rays after their discoverer (x-rays are named Röntgenstrahlung in German) [2]. (b) X-ray scattering image of the simple cubic ZnS crystal made by Friedrich, Knipping, and von Laue proving that x-rays are electromagnetic waves [3].

But x-rays paved the way into the quantum world as well. Inspired by Röntgen in 1912, Friedrich, Knipping, and von Laue performed the first x-ray diffraction experiment [3–5] unravelling the structure of crystals (figure 1.1b) and showing that x-rays are electromagnetic waves with small wavelengths in the order of the separation of atoms in a crystal.

Having now the possibility to disperse the x-ray emission from excited elements using the atomic layers of crystals [6] Moseley was able to prove the atomic structure proposed by Bohr [7] for heavier elements than hydrogen [8] establishing what we call today x-ray fluorescence analysis.

Modern applications of x-rays are still used to examine the electronic structure of atoms, molecules and cluster as well as the crystallise structure of complex solid states like high temperature su-

This project has received funding from the *European Union's Horizon 2020 research and innovation programme* under grant agreement No 654220.

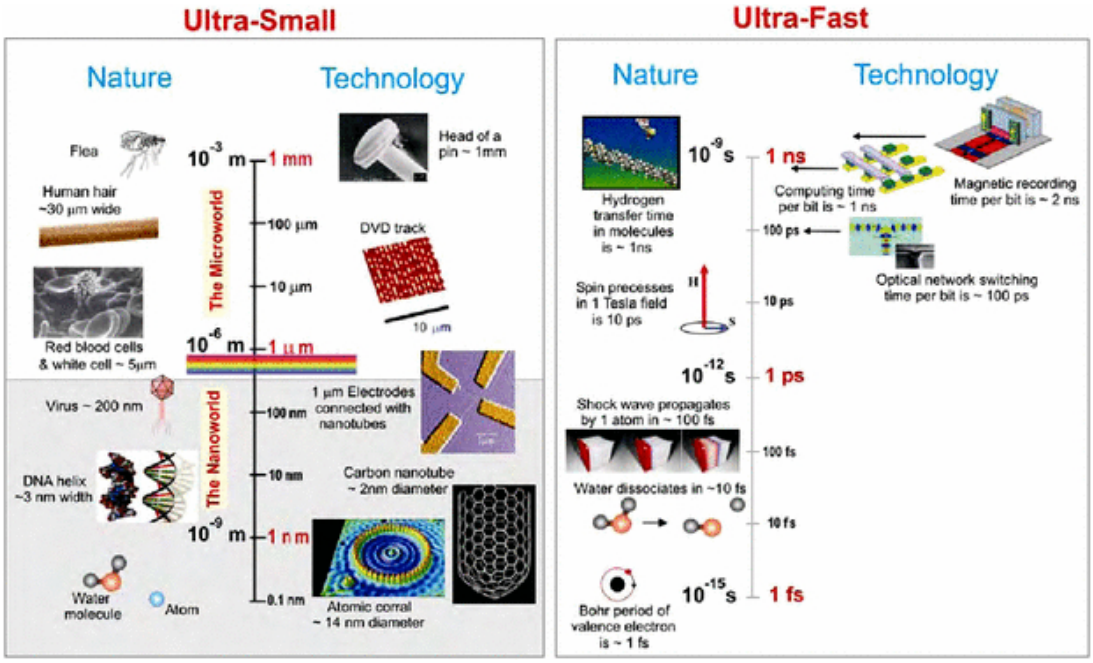

Figure 1.2: Scheme of size and time domains in nature and technology [34].

per conductors or large (bio-)molecules.

Intense and short pulse radiation became available with the upcoming lasers starting in 1960 with the ruby laser of Maiman [9]. But lasers were limited to the infrared and optical regime at first until the scheme of the production of higher harmonics (HHG) was established in late 1980s and early 1990s [10–12]. The production of soft x-rays was not reported before the 21st century [13].

Short pulses of light to examine atomic or molecular processes by pumping and probing were already used at end of the 19th century by Abraham and Lemoine switching a spark discharge with a Kerr cell [14]. An approach used in modern lasers for Q-switching as well but now reaching pulse widths of nanoseconds [15, 16]. The technique itself is even older. Töpler measured sound waves with two delayed spark discharges in 1867 [17].

Atomic, molecular and chemical dynamics reach from the nanosecond time regime down to the attosecond regime [18] therefore when short pulse intense lasers became available, great efforts were made to obtain ever shorter laser pulses. Picosecond pulses were reached using the mode-locking technique in 1966 [19], shortly followed after by sub-picosecond pulses generated with dye-lasers [20–23]. With the development of the Ti:sapphire laser by Moulton [24, 25] the pulse duration reached the femtosecond time regime [26–29] where it is possible to observe chemical reactions [18, 30]. After almost 100 years of getting light pulses ever shorter the attosecond time regime was reached [31, 32] down to a single cycle of a light pulse [33].

Figure 1.2 shows that tabletop lasers are able to examine the time domain of atomic and molecular processes interesting in nature and technology, but they cannot resolve the lateral

This project has received funding from the *European Union's Horizon 2020 research and innovation programme* under grant agreement No 654220.

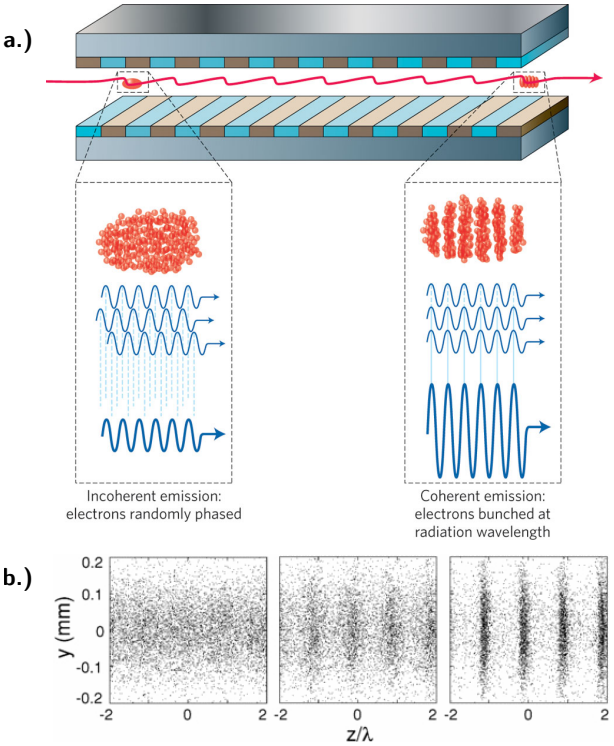

Figure 1.3: a.) Illustration of the microbunching of an electron bunch travelling through an undulator of a high-gain SASE FEL [52]. b.) Simulation of the density modulation of an electron beam in an FEL undulator showing microbunching [34].

dimensions. For this x-rays are required. X-rays were available at synchrotron storage rings but they lack the time structure generating pulses in the picosecond regime [34].
There have been concepts proposed to extend the laser principal into the x-ray regime [35–37] but they have not succeeded due to the required scaling of the pumping power to gain population inversion, the short lifetime of the levels involved and the low reflectively of the optics at hand [38, 39].
Because no high quality optics for x-ray cavities are available [40] the laser amplification has to be reached in one single pass through the active media. Beside some success using a plasma as an active medium [41], the active medium of choice to generate lasing of x-rays is a beam of electrons in a periodic magnetic field (undulator) as proposed and demonstrated by [42, 43]. For short x-ray pulses produced by such a free electron laser (FEL) relativistic electrons of high brilliance are needed which were developed during the 1980's [44–47]. Free electron lasers started to work in the XUV range [48] and the visible range of the electromagnetic spectrum [49] until the machines reached the soft x-ray range [50, 51] at the beginning of the 21st century. A topical review can be found in [52].

In the state of the art version of a FEL, electrons are accelerated in a linear accelerator to relativistic velocities producing x-ray radiation in an undulator up to saturation in a self am-

This project has received funding from the *European Union's Horizon 2020 research and innovation programme* under grant agreement No 654220.

plification by stimulated emission (SASE) scheme (see e.g. [34, 53–55]). The original electron distribution in the electron bunch is determined by the shot noise during the creation of the electrons. Upon entering of the electron bunch into the FEL undulator the bunch begins to emit spontaneous radiation which propagates ahead of the bunch generating a periodical electromagnetic field. The electron bunch starts to interact with its own field and gets more and more structured by it (see figure 1.3). The more this microbunching evolves the better is the coherent interaction between the bunch and the x-ray field yielding to an exponential growth of the radiation intensity until the bunch is fully structured or the undulator ends and the bunch is dumped. Because of this self amplification of the first stimulated emission of the random distributed electrons of the bunch at the beginning of the undulator each pulse produced in the SASE process is unique in its properties, like intensity, pulse length and, within the bandwidth of the undulator, photon energy, and not correlated with its predecessor or its successor.
The information gained in spectroscopic or scattering experiments depends on the knowledge of the properties of the excitation radiation therefore the diagnosis of FEL pulses is crucial. Because their properties are random and independent of each other it isn't sufficient to analyse a portion of the bunches and extrapolate. Each pulse has to be analysed in a non-destructive manner to know its properties and than the pulse has to be delivered to the experiment to be used.

This project has received funding from the *European Union's Horizon 2020 research and innovation programme* under grant agreement No 654220.

1.1 European X-Ray Free Electron Laser (European XFEL)

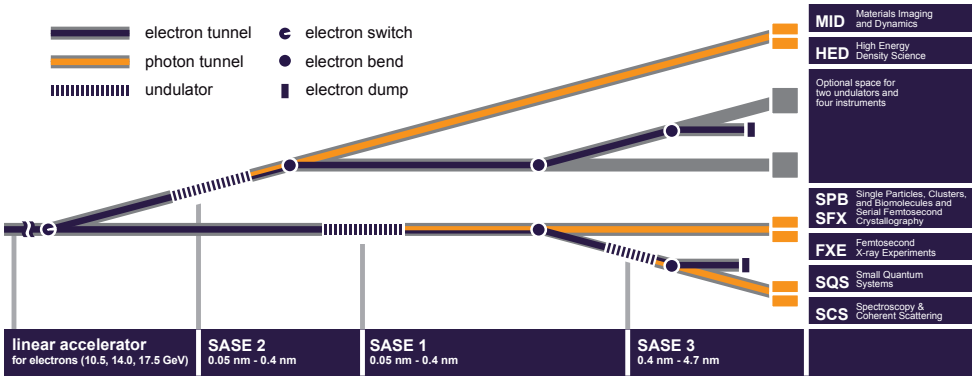

Figure 1.4: Illustration of the setup of the different undulator beamlines and dedicated experiments of the European XFEL [56].

The European X-Ray Free Electron Laser (European XFEL) is cryogenic cooled linear accelerator (linac) based SASE free electron laser dedicated to produce short x-ray pulses from the soft to the hard x-ray regime of the electromagnetic spectrum [54]. The experiments settled at three different undulators are:

MID Materials Imaging and Dynamics to study the dynamic fluctuations of matter on time and length scales so far not accessible.

FXE X-ray Femtosecond Experiments to study ultra-fast processes in solids, liquids, and soft-matter.

HED High Energy-Density Science to produce and study warm dense matter.

SPB Single – Particle, Cluster and Biomolecular Imaging of single (bio-)molecules and clusters

SQS Small Quantum Systems. Gas phase spectroscopy on atoms, molecules, and ions at high field stregnth.

SCS Soft X-ray Coherent Scattering and Spectroscopy including resonant inelastic x-ray scattering (RIXS), fluorescence and photoelectron spectroscopy.

and are dedicated to time-resolved studies of sub-picosecond dynamics, structural imaging of single (bio-)molecules or clusters, non-linear x-ray optics, and warm dense matter.

Figure 1.4 gives an overview of the setup of the European XFEL and the operation parameters (table 1.1) of the different SASE beamlines delivering the x-ray photons to the experiments. The linac can be operated up to 17.5 GeV to generate x-ray photons in three different SASE undulators between 0.05 nm to 4.7 nm wavelength or 260 eV to 25 000 eV energy respectively [54,

This project has received funding from the *European Union's Horizon 2020 research and innovation programme* under grant agreement No 654220.

57]. The RF gun producing the electron bunches for acceleration will be able to produce up to 27 000 pulses per second. Fast switches will make it possible to distribute the electron bunches to different SASE beamlines operating more than one experiment at a time. The minimum spacing between the 2700 x-ray pulses of one bunchtrain will be 220 ns (4.5 MHz repetition rate) [54].

maximum electron energy	17.5 GeV
photon wavelength	0.05 nm to 4.7 nm
photon energy	260 eV to 25 000 eV
number of photons per pulse	$\approx 1 \times 10^{12}$
peak brilliance	5×10^{33} photons/s/mrad^2/mm^2/0 1%BW
pulses per second	27 000 at 4.5 MHz in 10 bunchtrains
spot size (FXE)	user defined: either below 30 µm
	or in the range of 100 µm to 250 µm

Table 1.1: Operation parameters of the European X-Ray Free-Electron Laser (European XFEL) according to [54, 58].

This project has received funding from the *European Union's Horizon 2020 research and innovation programme* under grant agreement No 654220.

1.2 Extreme Light Infrastructure (ELI)

The Extreme Light Infrastructure (ELI) [59, 60] is the European initiative to provide light sources for users to produce pulses with energies up to the EW (1×10^{18} Watt) regime and as short as ranging from fs (1×10^{-15} s) to zs (1×10^{-21} s) pulse length. The scientific case of ELI covers studies in high energy, vacuum, and extradimensional physics, light matter interaction in the ultra-relativistic regime at an irradiance above 1×10^{24} W cm^{-2}, as well as applications in oncology, (bio-)medical and fast electronics imaging. ELI is divided in three different sites hosting different specialised experimental set-ups for user operation:

ELI Nuclear Physics (NP) hosted in Magurele, Romania, will provide ultra-intense optical and gamma ray pulses for studies in nuclear physics and its application.

ELI Attosecond Light Pulse Source (ALPS) hosted in Szeged, Hungary, will provide attosecond and shorter pulses with high repetition rate to achieve best time resolution to study the electron dynamic of atoms and molecules.

ELI Beamlines hosted near Prague, Czech Republic, will provide short x-ray pulses either in a higher harmonic generation (HHG) scheme or in an undulator with a wakefield accelerator and particle beams in general.

The context of the report will concentrate on ELI Beamlines because these groups are part of PUCCA, but the methods proposed can be applied by ELI-NP or ELI-ALPS as well.
The experimental set-up of ELI Beamlines can be see in figure 1.5. An overview of the laser parameter is given in table 1.2 and an overview of the secondary sources for x-rays are given in table 1.3.

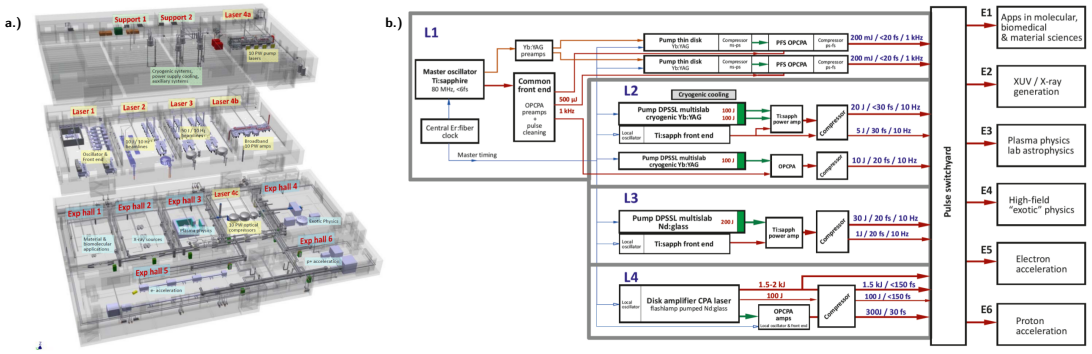

Figure 1.5: Schematics of (a) the set-up of ELI Beamlines with the different laboratories dedicated to different user applications: material and biomolecular studies, x-ray spectroscopy, plasma physics, exotic physic, and electron and proton acceleration and (b) the different laser systems available for users [60].

This project has received funding from the *European Union's Horizon 2020 research and innovation programme* under grant agreement No 654220.

The scientific case of ELI Beamlines include five different research programs utilising different laser concepts like lasers generating high repetition rate ultra-short pulses and multi-petawatt peak power (RP1), lasers driving high repetition rate x-ray sources (RP2), lasers for wakefield particle acceleration (RP3), lasers for the application in material, molecular and biomedical science (RP4), and lasers for plasma generating and high-energy-density physics (RP5). To drive these different programs four different laser beamlines will be established ranging in pulse energy from 5 mJ to above 1.5 kJ with repetition rates in the range of 1 kHz (10 Hz for the high energy laser) and a pulse duration in the order of 30 fs (below 3 ns for the high energy laser). All four lasers can be focused down to a 4 µm spot size [60].

	laser L1	laser L2	Laser L3	laser L4
repetition rate	1 kHz	<1 kHz	<1 kHz	<10 Hz
pulse energy	5 mJ to 10 mJ	5 J	15 J	>1.5 kJ
pulse duration	30 fs	30 fs	30 fs	<3 ns
focus diameter	4 µm	4 µm	4 µm	4 µm

Table 1.2: Operation parameters of the four different laser beamlines L1 to L4 driving the experiments in the experimental halls 1 to 6 of ELI beamlines [60].

The four laser beamlines L1 to L4 will drive different secondary light sources to generate x-ray pulses between 100 eV and 1 MeV photon energy (see table 1.3) like a high harmonic generation (HHG) source, a K_α source, a betatron source and an inverse Compton scattering source. The x-rays can be used for scattering experiments on solids or (bio-)molecules, for time resolved or coherent diffration imaging, or ultra-fast soft or hard x-ray spectroscopy [60].

photon wavelength	0.001 nm to 10 nm
photon energy	100 eV to 1 000 000 eV
number of photons per pulse	1×10^4 to 1×10^6
pulse duration	10 fs to 100 fs
spot size	2 µm to 600 µm
repetition rate	1 kHz or <10 Hz

Table 1.3: Summary of the operation parameters of the different x-ray sources of ELI Beamlines driven by its laser beamlines L1 to L4 (see table 1.2) [60].

This project has received funding from the *European Union's Horizon 2020 research and innovation programme* under grant agreement No 654220.

1.3 Goals of the Workpackage Pulse Characterisation and Control (PUCCA) within the EUCALL framework

To control the machine and the experiments as well as interpret the data obtained by them, the characteristics of any light source must be known. Ideally these characteristics are measured before the pulse is used by the experiment because the interactions studied can cause changes to the pulse, for example during a scattering experiment. One strategy to analyse the pulses before the experiment can be to take away some of the pulses of the source, analyse them and extrapolate the measured properties to any other pulse. This approach works for light sources producing uniform pulses like lasers, but won't work for the statistical nature of the SASE process of FELs. Here one has to analyse shot-by-shot each single pulse non-destructively to determine its properties and document them for the user experiment.
The properties of the pulse which must be known to users are its photon energy/wavelength, its pulse intensity, and its pulse length. Scattering experiments have to know additionally the wavefront of the light pulse after travelling through all optical elements of the beamline and if an external visible or infrared laser is combined with the x-ray pulse to perform a pump-probe experiment the jitter between the two pulses must be known.
Within the pulse characterisation and control (PUCCA) workpackage of EUCALL joint approaches for the diagnostic of the pulse intensity, the measurement of the pulse wavefront and the determination of the jitter between an optical and a x-ray pulse, for laser based and FEL x-ray sources will developed. As can be seen for the operation parameters of the European XFEL (table 1.1) and for the parameters of the secondary x-ray sources of ELI Beamlines (table 1.3), the values for characteristic parameters for the different sources are spanning several orders of magnitude. To provide tools for a general approach of the diagnostic of these sources is the main goal of PUCCA.
The report at hand will concentrate on techniques to determine the pulse intensity of an x-ray source. The specific goals for the intensity monitor have been defined in the EUCALL proposal [61] as:

Task 7.3.1 Analysis of x-ray intensity monitors based on gas ionisation (DESY): study of the ultimate uncertainty achievable with transparent intensity monitors (based on the statistics of ionisation events) for the different FEL and ELI sources; design study of optimised intensity monitors based on the present design for XFEL.

Task 7.3.2 Construction and test of a prototype x-ray intensity monitor (DESY). The prototype will be optimised for intensity measurements of hard x-rays with ultimate precision, i.e. the most difficult application of this monitor concept. Absolute calibration at PTB (Physikalisch-Technische Bundesanstalt); test at XFEL (if available) or LCLS; measurements at ELI sources and other FELs as much as possible.

This project has received funding from the *European Union's Horizon 2020 research and innovation programme* under grant agreement No 654220.

Beside the tasks set within the workpackage a user survey was organised at the poster sessions during the FS user meeting 2016 in Hamburg and during the DPG spring meeting 2016 in Hannover. The participants of the survey indicated the following desired features::

- simple working small GMD after experiment for verification of beam intensity
- miniature GMDs for beam splitter branches (SDUs)
- good signal-to-noise ratio at 14keV
- sensitive for polarisation
- fast output for data rejection (vetoing) with 2D detectors at European XFEL
- compact design for lasers
- device for temporal overlap and jitter correction (or at least jitter measurement) between laser and FEL installable at each of the beamlines (fs resolution <20fs)

The result of the survey can be summarised as the users are looking for a simple, robust and especially compact design for a x-ray intensity detector. Not all needs can be addressed by an intensity monitor, but all needs are addressed within the frame of PUCCA.

This project has received funding from the *European Union's Horizon 2020 research and innovation programme* under grant agreement No 654220.

2 Methods of x-ray pulse diagnosis

For photon diagnosis the interaction of light with matter is utilised, mainly the photoelectric effect discovered by Hertz [62] and explained by Einstein [63]. Depending on the state of the matter used, it is distinguished in an outer photoionisation process exciting electrons into vacuum from a gas phase (atomic) target, or an inner photoionisation exciting electrons from the valence band into the conduction band of a solid, mostly a semiconductor.
The observables for the outer photoionisation are electrons, ions, or fluorescence photons. Information of the exciting photon can be gained by analysing the kinetic energy of the photo-excited electron reaching the vacuum, the charge state of the residual (atomic) ion, or the wavelength of the fluorescence photon. Additional information can be determined by the angular distribution of the photoelectrons or the polarisation of the fluorescence photons. An overview of the spectroscopy techniques and information available in photoionisation of atomic targets is given in [64].
The observable exploiting the inner photoionisation in e.g. a semiconductor is usually the number of electrons excited from the valence to the conduction band which can be counted by an electronic logical circuit connected to the semiconductor. Knowing the band gap the exciting photon energy and intensity can be determined.
All these methods depend upon the knowledge of the electronic structure of the target used and can only as precise as this.

2.1 Gas Phase Detection Methods

Photoionisation detecting charged particles in the gas phase is successfully exploited at FEL facilities like FLASH I [65–67], FLASH II [68, 69], and FERMI [70, 71], or will be used as in the case of the European XFEL [54, 72, 73]. The LCLS uses gas monitors as well, but detects fluorescence photons instead of particles [74].

This project has received funding from the *European Union's Horizon 2020 research and innovation programme* under grant agreement No 654220.

Using photoemission to measure the intensity of radiation, the basic relation between the number of incident photons N_{ph} and the number of particles created N_e can be written as [75]:

$$N_e = N_{ph} \cdot n \cdot \sigma(\hbar\omega) \cdot l \tag{2.1}$$

n : *density of the gas phase target in the interaction volume*
$\sigma(\hbar\omega)$: *photon energy dependent cross section of the gas phase target*
l : *effective absorption length of the interaction volume along the photon beam axis*

To optimise the particle yield improving the number of created charged particles N_e, and hence the counting statistic, all three technical parameters, the target density n, the cross section $\sigma(\hbar\omega)$, and the absorption length l, in equation (2.1) can be improved. But all improvements gaining more particles N_e for counting have their specific drawbacks which have to be considered in the design of the detector.
The target density n can be optimised by increasing the partial pressure of the target gas. But to be able to operate open multipliers or multi-channel plates (MCPs), which are sensitive for low particle numbers N_e as well, the partial pressure of the vacuum chamber in the area of the detector has to be kept in a range below 1×10^{-3} hPa. Hence heavy pumping is needed, which increases the costs of the vacuum chamber.

Typically noble gas atoms are used as targets for photoemission for photon diagnostics, because their cross section $\sigma(\hbar\omega)$ is well studied and tabulated ([75] and references therein) and they are chemically harmless and as such easy to handle. But as can be seen in figure 2.2, the absorption cross section $\sigma(\hbar\omega)$ depends on the excitation energy $\hbar\omega$ of the photons. Changing the excitation energy into the hard x-ray regime the cross section of the rare gases drops by several orders of magnitude compared to the soft x-ray regime hence reducing the particle yield and increasing the statistical uncertainty.

Optimising the absorption length l, in principal, any detector can be build as large as to bring the counts N_e into the desired order of magnitude. But in most cases the laboratory space is limited hence limiting the dimensions of the detector. On the other hand, there are special applications where a miniaturised version of a non-destructive intensity monitors is needed. Regarding for example a beamsplitter [78, 79], to control the measurement, place one beam intensity monitor in each arm of the beamsplitter to control the intensity distribution of the splited pulses.
Based upon photoionisation of noble gases in a collaboration DESY, the Ioffe-Institute and the Physikalisch-Technische Bundesanstalt (PTB) Berlin developed a gas monitor detector (GMD) [75] to analyse the intensity of the FLASH soft x-ray pulses on absolute scale. The main detectors of the GMD are two Faraday Cups facing each other (figure 2.1). Between the two Faraday Cups a high electric field is applied separating the photoelectrons from the photoions reaching

This project has received funding from the *European Union's Horizon 2020 research and innovation programme* under grant agreement No 654220.

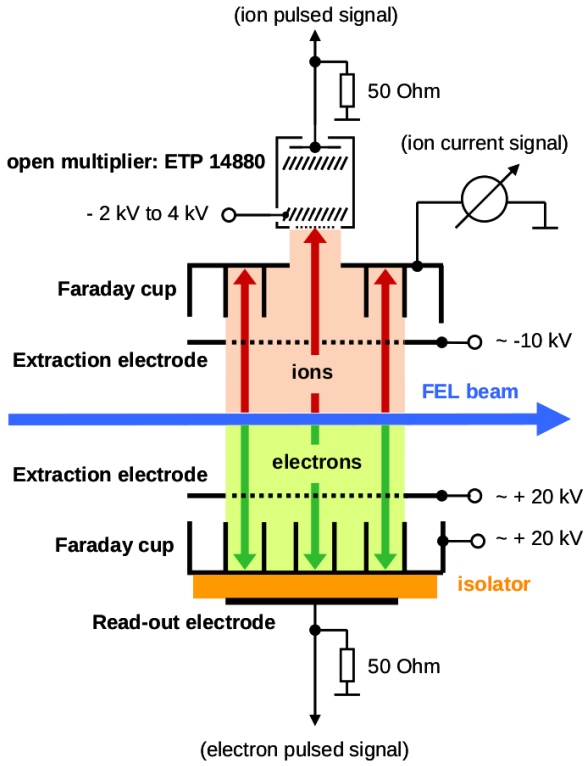

Figure 2.1: Scheme of the FLASH GMD. Photoelectrons and -ions produced by photoionisation of noble gas atoms are separated via a constant electric field and collected by two Faraday Cups facing each other. In the middle of the ion Faraday Cup is an aperture leading to a photomultiplier working as a time-of-flight spectrometer analysing the mass-to-charge ratio of the photoions [76].

opposite Faraday Cups. The Faraday Cup for the photoions includes in addition a time-of-flight drift tube with an open multiplier to be able to analyse the mass-to-charge ratio of the photoions. The target rare gas pressure is measured by a spinning rotor gauge and controlled by an automatic gas inlet valve. The temperature of the chamber and gas inlet is measured by a calibrated PT100 sensor. From these information, the target density can be determined from the ideal gas equation.

With this, all values of the variables of equation (2.1) are known and hence the intensity of the photon beam N_{ph} on absolute scale.

The set-up is able to handle 800 bunches per second in 10 bunchtrains, detecting the intensity of each bunch by individually collecting the fast photoelectrons created by each bunch. To normalise the fast signal of the electrons to absolute scale, the slower ions are measured over many bunchtrains. The detection efficiency of the ion Faraday Cup was calibrated at the Metrology Light Source (MLS) of the PTB Berlin [80–82]. The intensity of an single bunch of FLASH can be determined by the GMD with an uncertainty below 10 % [75].

This project has received funding from the *European Union's Horizon 2020 research and innovation programme* under grant agreement No 654220.

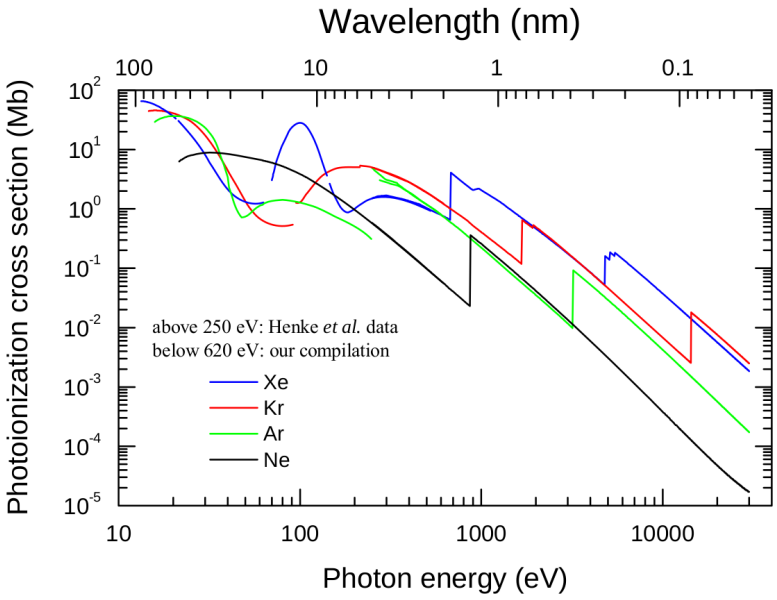

Figure 2.2: Cross section of the noble gases from the soft to the hard x-ray regime of the electromagnetic spectrum [76, 77].

It has been demonstrated that the GMD works in the hard x-ray regime [76] as well as with pulses of low intensity of an laser HHG source [83].

2.2 Photodiodes

Photodiodes are semiconductors, mostly silicon, with parts which are positively (p) and negatively (n) doped with materials from the 3^{rd} and 5^{th} main-group of the periodic table. At the barrier between the p-doped and n-doped area (p-n junction) of the photodiode, photons can create electron-hole pairs via the inner photoeffect. These pairs diffuse to the electrically connected sides of the photodiode and there are detected as current. The p-n junctions dates back to works of Rother and Bomke [84] who examined copper-oxide layers, and of Lashkaryov [85] and Ohl who got the patent for the photodiode in 1946 [86].
Photodiodes are compact, easy available, easy to handle and their average response time of 200 ps is fast enough to handle the pulse repetition rate of the European XFEL (see e.g. [87, 88] and table 1.1). But photodiodes are usually not transparent absorbing all the photons hence they have to be placed behind a user experiment. In addition, they suffer from radiation damage if used above the UV range (see e.g. [89]). Nonetheless, photodiodes are used as detectors in VUV range [90], the EUV range [91] and the x-ray range [92–94] of the electromagnetic spectrum. Great effords have been made to calibrate photodiodes to measure the photon flux on absolute scale using a synchrotron storage ring as primary standard [80–82, 95, 96].

This project has received funding from the *European Union's Horizon 2020 research and innovation programme* under grant agreement No 654220.

2.3 Bolometer

The primary standard for the determination of the intensity of radiation are bolometers [81, 82, 95]. The energy of the incident radiation is dumped in a cavity which is isolated from its surrounding. The change of temperature due to the absorbed radiation is proportional to the energy dumped into the cavity and by measuring the temperature, the intensity of the incident radiation can be determined.
Usually, for high sensitivity, cryogenic bolometers are used [81, 97, 98], but an improved version can be operated at room temperature (see figure 2.3) [99, 100]. Here, the absorber is kept on a constant temperature by an electric driven heat wire controlled by a temperature sensor. Upon incident radiation the temperature rises and less electric current is needed to heat the absorber to keep the temperature constant. The change in the electric current is linear to the incident radiation and can be measured with an electrometer [99, 100].
Measuring temperature is considered to be slow, in the order of some few seconds [98, 100], but using sophisticated electronics, bolometers can measure single x-ray pulses shot-to-shot [101] at a repetition rate of 20 Hz [102]. Because bolometers absorb all the radiation of the FEL beam to measure its intensity, they can not be used as beamline infrastructure before the experiment. As photodiodes, they have to be placed behind the user experiment.

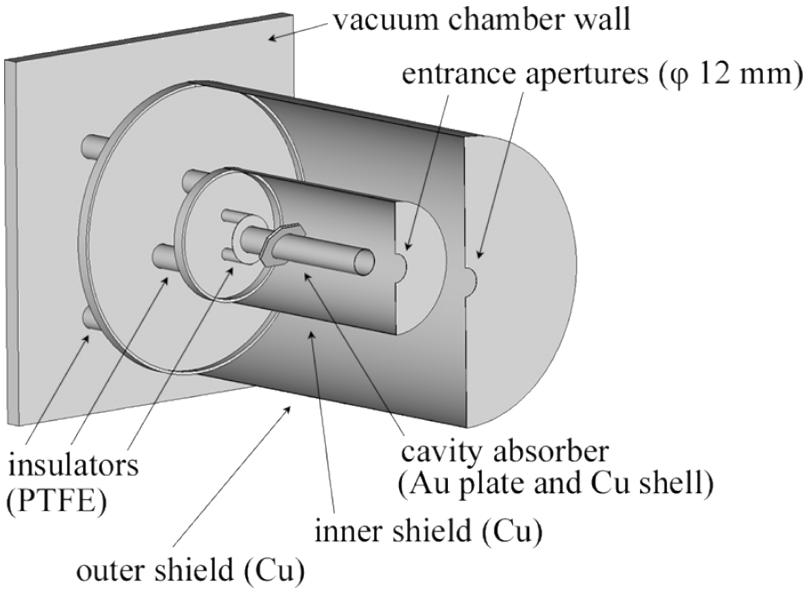

Figure 2.3: Scheme of the room temperature bolometer of SCALA, Japan [99].

This project has received funding from the *European Union's Horizon 2020 research and innovation programme* under grant agreement No 654220.

3 Design Study of a Gas Monitor Detector for ELI and European XFEL

As summarised in the tables 1.1 and 1.3 the operation parameters of the European XFEL and ELI Beamlines span several orders of magnitude. Especially, the number of photons per pulse differs largely which is the key quantity for the determination of the intensity. As pointed out in equation (2.1) there are several technical parameters, like the target gas density n or the effective absorption length l, which can be optimised to detect a presumed weak signal. In addition, reaching the limit of single particle detection, multiplier stages are needed to amplify the signal. But open multipliers limit the target gas pressure where they can be operated.
Based upon the layout of the gas monitor detector (figure 2.1) introduced in section 2.1, a "huge aperture open multiplier" (HAMP) will be described for the determination of the intensity of a x-ray pulse of either a low number of photons per pulse or a low cross section of the gas used as target material.

The dimensions of the active multiplier surface will be 100 mm in direction of the x-ray beam propagation and 20 mm wide (figure 3.1). The dimensions of the detector are small enough it can be housed on a CF160 flange [103] which is compliant with the DESY specifications [104] and commercial easily available. The open multiplier itself will consist of several dynode stages for secondary particle amplification made of solid material to be able to operate it with high target gas densities n.
Along the axis of the dynodes from the interaction volume to the anode a high voltage for charged particle acceleration will be applied to guide all created particles from the interaction volume to the anode. The high voltage will be applied to the dynodes by a passive voltage divider with a total resistance of several MΩ being able to use only one high voltage power supply. Special care will be taken to shield external magnetic fields from the multiplier, for example surrounding the hole set-up with a Mu-metal shielding.
A possible schematic setup of an improved gas monitor detector for ELI and the European XFEL is depicted in figure 3.1. The created primary photoelectrons and photoions are separated by a constant electric field accelerating the primary particles to opposite Faraday Cup type detectors. The high acceleration voltage of 20 kV ensures the drift time of the electrons from the interaction volume to the anode is below 200 ns corresponding to the maximum repetition rate of x-ray pulses of the European XFEL of 4.5 MHz (see table 1.1). The electron signal will

This project has received funding from the *European Union's Horizon 2020 research and innovation programme* under grant agreement No 654220.

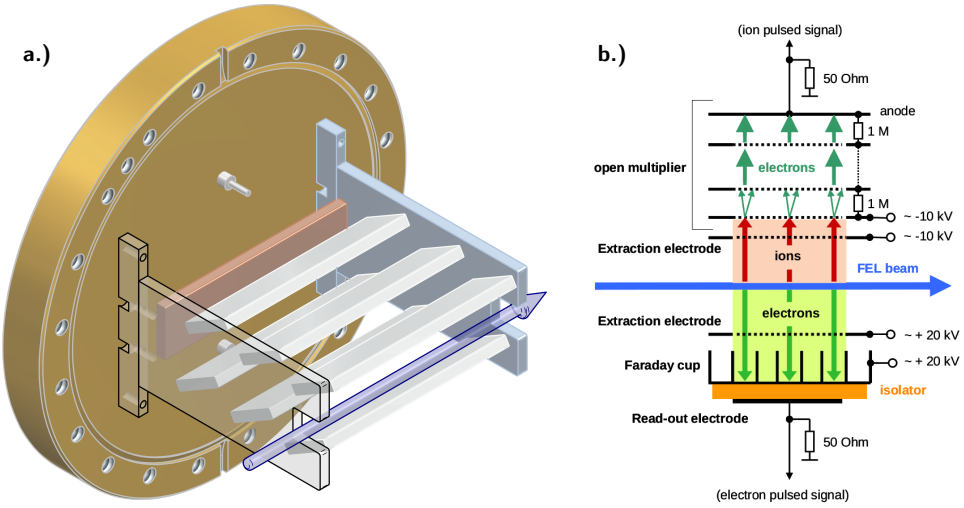

Figure 3.1: (a) CAD model of the "huge aperture open multiplier" (HAMP) detector sitting upon a CF160 flange. The dynodes are solid material to be able to operate it at high target gas densities. Only the ion detection part is shown. (b) Sketch of an improved gas monitor detector for low signal amplification based upon HAMP. The created primary charged particles are separated by a constant electric field towards two Faraday Cup type detectors facing each other. The fast electron signal can be used to determine the pulse intensity shot-by-shot. The slower photoions are converted and amplified by dynodes into an secondary electron avalanche.

therefore be able to detect the photon pulse energy of each individual pulse. The slow photoion signal for the calibration of the photon pulse intensity to absolute scale will be amplified by the dynode stages of HAMP to be able to detect pulses with a low number of photons. According to equation (2.1) for the operation parameters of the European XFEL (table 1.1) and a minimal number of photons per pulse of $N_{ph} = 1 \times 10^{12}$:

$$N_{ions} = N_{ph} \cdot \frac{p}{kT} \cdot \sigma(\hbar\omega) \cdot l \tag{3.1}$$

$$N_{ions} \approx 500 \tag{3.2}$$

$N_{ph} = 1 \times 10^{12}$	*: number of photons of of pulse*
$p = 1 \times 10^{-7}$ hPa	*: target gas pressure in the chamber*
k	*: Boltzmann constant, see e.g. [105]*
$T = 300$ K	*: room temperature*
$\sigma(\hbar\omega) = 2.1 \times 10^{-24}$ m^{-2}	*: cross section of xenon at* 12.4 keV *photon energy (see figure 2.2)*
$l = 0.1$ m	*: effective visible absorption length of HAMP*

approximately 500 ions can be created at an photon energy of 12.4 keV.

This project has received funding from the *European Union's Horizon 2020 research and innovation programme* under grant agreement No 654220.

For the operation parameters of ELI Beamlines (see table 1.3) it will be approximately:

$$N_{ions} \approx 5 \tag{3.3}$$

$N_{ph} = 1 \times 10^4$	*: number of photons of of pulse*
$p = 1 \times 10^{-4}$ hPa	*: target gas pressure in the chamber*
k	*: Boltzmann constant, see e.g. [105]*
$T = 300$ K	*: room temperature*
$\sigma(\hbar\omega) = 20 \times 10^{-22}$ m^{-2}	*: cross section of Xenon at* 100 eV *photon energy (see figure 2.2 or e.g. [64])*
$l = 0.1$ m	*: effective visible absorption length of HAMP*

5 ions created at 90 eV photon energy and an increased Xe target gas pressure of 1×10^{-4} hPa which is already above the common operation range of open multipliers. Furthermore, because of the low number of particles the detection scheme is benefiting of an even higher target gas pressure hence the dynode material and layout has to be robust against electric discharges. Especially for the ELI case an amplification factor of at least 1×10^{10} is needed to reach the pA level necessary for readout with an electrometer.

3.1 Improvement and Characterisation of the open Multiplier

The key feature of HAMP will be the solid dynodes exploiting their customisable high secondary electron yield δ [106, 107] to amplify even low signals either because of less photons per pulse or because of a low cross section of the detector target gas. The amplification will not improve the uncertainty caused by counting statistics, but the detector will give information even if only a single particle is created by the x-ray pulse.

Almost all metals of the periodic table have been investigated on their property of secondary electron emission and its dependency of the voltage between the dynode stages (see i.e. the review of Walker *et al.* [106]). For HAMP metals, most suitable are those, which are UHV compatible and cheap. Best are Al, Cu, or Fe of stainless steel, but to make the HAMP robust against discharges caused by high target density, the voltage between the dynodes have to be as low as possible and at the same time the secondary electron yield of amplification as high as possible. The dependence of secondary electron yield δ on the voltage between the dynodes of possible candidate materials are shown in figure 3.2.

As can be seen at the different values for δ between the curves of fresh samples (x in figure 3.2) and cleaned samples (+ in figure 3.2) oxidisation of the surface plays an important role to tailor the amplification property of the different dynode materials. To clarify the impact of oxidisation as well as fatigue fretting, oxidised copper samples have been chosen as a model system and have been examined using x-ray absorption spectroscopy using the detection of

This project has received funding from the *European Union's Horizon 2020 research and innovation programme* under grant agreement No 654220.

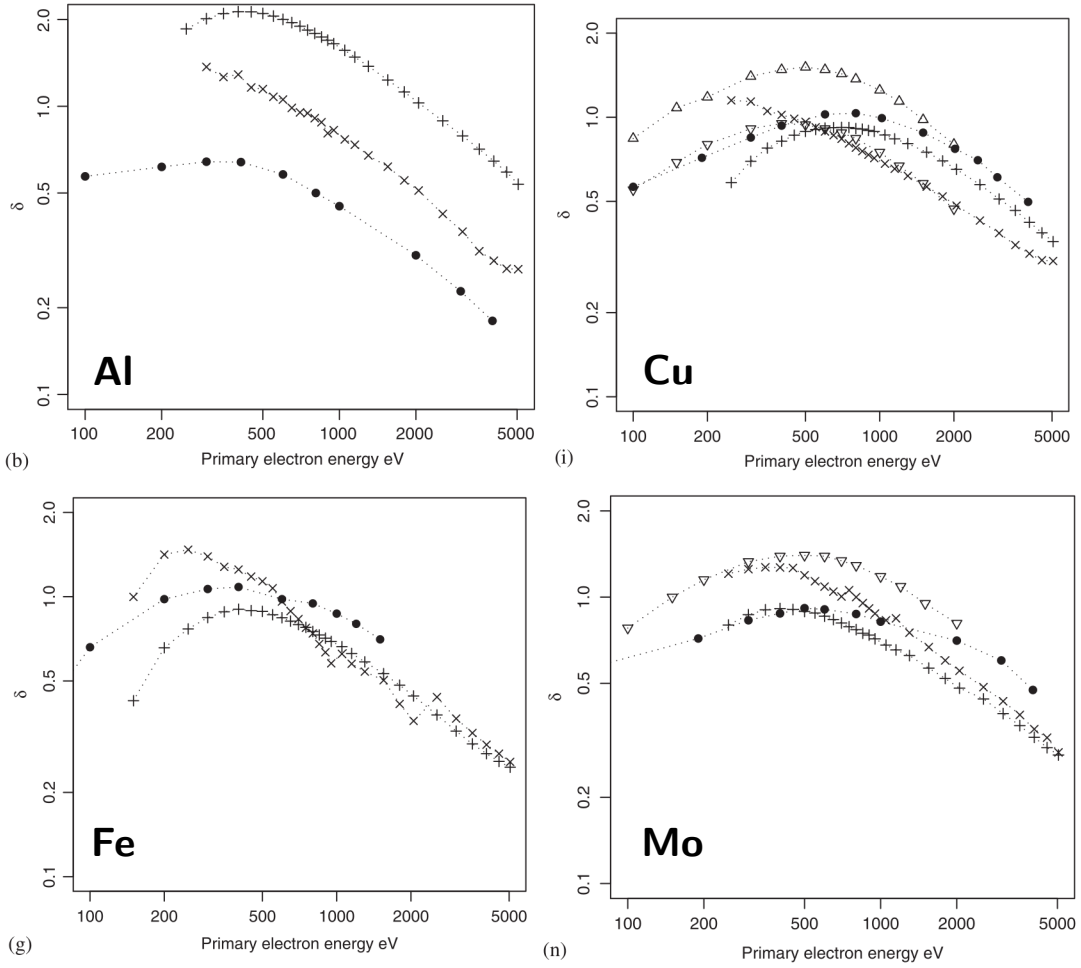

Figure 3.2: Secondary ion yield δ of (b) Al, (i) Cu, (g) Fe, and (n) Mo depending on the incident kinetic energy of the primary electron. The pictures and their labelling is taken from [106]. Curve symbols: (x) fresh sample, (+) cleaned sample, (•) data from [108], (∇) and ($\triangle$) data from [109]

the total electron yield after photoemission. The x-ray photons have been delivered by the soft x-ray beamline P04 [110], PETRA III, DESY, scanning the excitation range of the Cu L-edge (see figure 3.3) and the O K-edge (see figure 3.4).

As can be seen in figure 3.3 and figure 3.4 the oxidisation and especially ageing have a significant impact on the electronic structure of the oxidised Cu. This is most prominently seen in the measurement of the O K-edge (figure 3.4). There even vanishes the absorption feature before the absorption edge after letting the sample rest at air.
The data haven been taken recently in June 2016 hence the results are preliminary at the present stage and have to evaluated more carefully.
The measurements have to be extended to the materials of figure 3.2 as well and the quality

This project has received funding from the *European Union's Horizon 2020 research and innovation programme* under grant agreement No 654220.

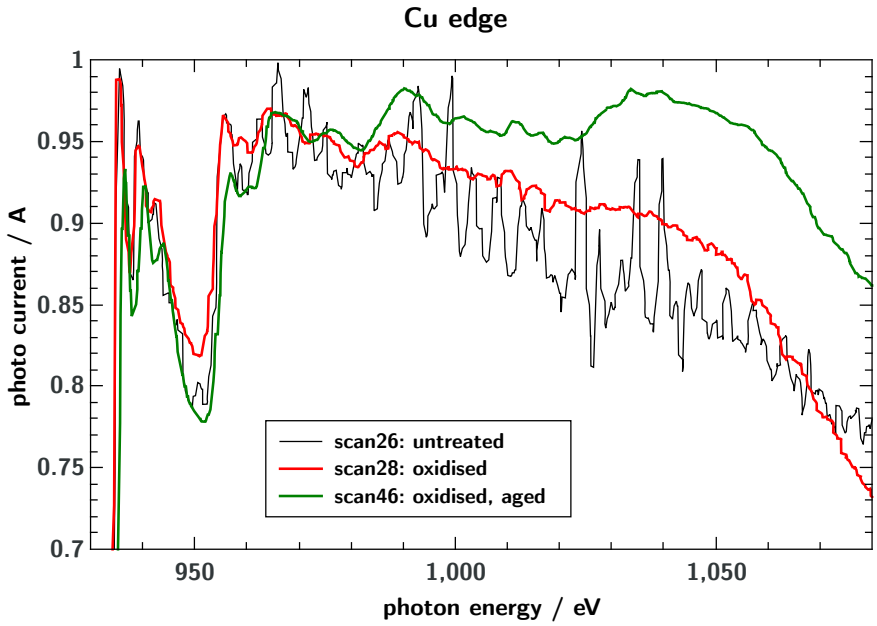

Figure 3.3: Absorption spectra of oxidised Cu in the excitation photon energy range of the Cu L-edge.

of the data has to be improved in a dedicated beamtime at P04 in 2017.

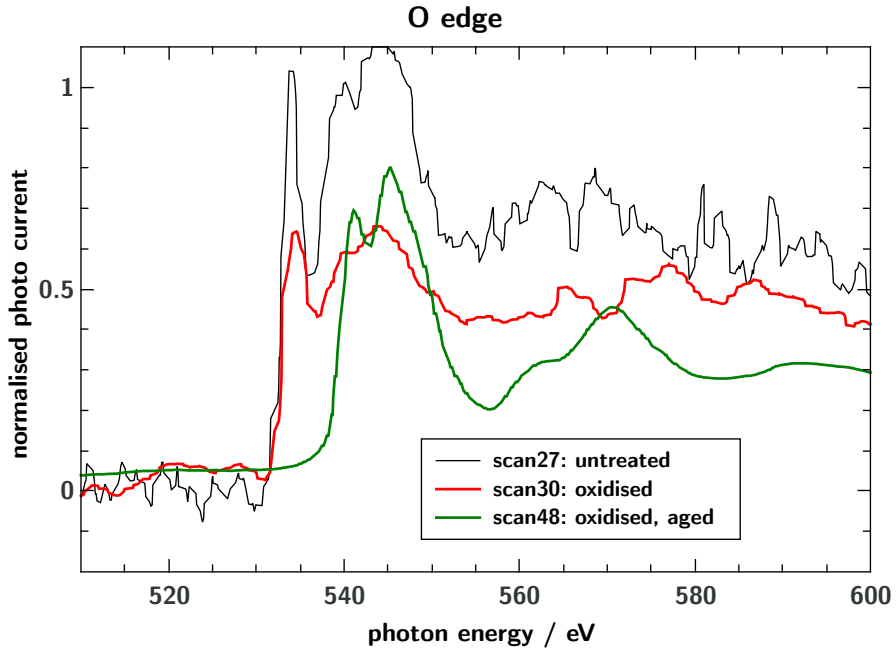

Figure 3.4: Absorption spectra of oxidised Cu in the excitation photon energy range of the O K-edge.

This project has received funding from the *European Union's Horizon 2020 research and innovation programme* under grant agreement No 654220.

4 Synergy Aspects

Light interacting with matter triggers a number of different processes like photoemission of electrons, Auger or fluorescence decay. The absorption of photons in matter can be described as (see e.g. the review [64]):

$$\sigma(\hbar\omega) = \frac{1}{nd} \cdot \ln\left(\frac{I(d)}{I_0}\right) \tag{4.1}$$

$\sigma(\hbar\omega)$	*: photon energy depended total absorption cross section*
n	*: target density*
d	*: target thickness*
$I(d)$	*: transmitted photon intensity depending on target thickness*
I_0	*: incident photon intensity*

The total absorption cross section $\sigma(\hbar\omega)$ includes in this picture all triggered processes within the target and embodies the probability to absorb a photon in the target of given density n and thickness d. To determine the value of the cross section, the intensity of the incident photons I_0 must be known. From the transmitted photon intensity $I(d)$ the value for I_0 can not be evaluated because in most scientific cases the value of the cross section is of interest. Both quantities can not be measured by the same target as can be seen in equation (4.1). Thus, it is crucial for spectroscopic experiments to determine the intensity of the incident photons I_0 before the target of the study.

Within PUCCA a transparent and robust incident photon intensity monitor (HAMP) will be provided to determine I_0 on absolute scale suited for FEL and lasers, but as well for synchrotron sources. In this context, HAMP will be able to resolve the statistical varying pulses of a linac driven FEL, like the European XFEL, on shot-to-shot basis as well as being able to amplify and measure the signal of a low intensity laser source, like e.g. the K_α source of ELI Beamlines. HAMP will provide the users of the named facilities with the information of the incident photon beam they need to interpret their data without the need to be aware of all of the details of the respective user facility.

This project has received funding from the *European Union's Horizon 2020 research and innovation programme* under grant agreement No 654220.

5 Conclusions

The operation parameters of the European XFEL and ELI Beamlines span several orders of magnitude (see table 1.1 and 1.3). Whereas the pulses of the optical lasers of ELI are uniform in shape, the pulses of the European XFEL vary because of shot-noise during the generation of the electron bunch shot-by-shot. The introduced concept of a "huge aperture multiplier" (HAMP) detector with several open dynode stages (see figure 3.1) will address the specific needs of both facilities. In particular, the HAMP detector will be fast enough to analyse the photon pulses of the European XFEL shot-by-shot with a repetition rate of 4.5 MHz while it will be sensitive enough to register pulses as weak as 1×10^4 photons per pulse.

This project has received funding from the *European Union's Horizon 2020 research and innovation programme* under grant agreement No 654220.

6 Summary

In this work, the design of a transparent x-ray intensity detector is presented, which will be capable of non-invasively monitoring the pulses delivered by both the European XFEL as well as those at ELI Beamlines. The requirements for such a detector are particularly demanding, as within one pulse train the European XFEL will deliver pulses of x-rays every 200 ns in the energy range 0.26 keV to 25 keV, while at ELI Beamlines an energy range of 0.1 keV to 1000 keV is expected, although with a lower repetition rate. Furthermore the number of photons per pulse varies widely, with 1×10^{12} photons per pulse at European XFEL but only 1×10^{4} to 1×10^{6} photons per pulse at ELI Beamlines.

Current x-ray gas monitor detectors developed for UV and soft x-rays at FLASH and other FEL facilities will require extensive modification to be useful at European XFEL and ELI Beamlines. These detectors contain xenon gas, which release photoions and electrons upon interaction with x-ray/UV photons. We propose the integration of the "huge aperture open multiplier" (HAMP) detector which will guide and amplify the created charged particles by electrical fields to the point where they can be registered, to be able to detect the weak signals of an x-ray beam at ELI Beamlines as well as being fast enough to detect every single pulse of the European XFEL. With this transparent concept, using only small amounts of the pulse and amplifying the weak signal, it is possible to analyse the properties of the x-ray pulses before they reach the experiment, without having a significant effect on the pulse itself.

This project has received funding from the *European Union's Horizon 2020 research and innovation programme* under grant agreement No 654220.

Bibliography

[1] W. C. Röntgen, Annalen der Physik **300**, 1–11 (1898)
DOI: 10.1002/andp.18983000102.

[2] G. Landwehr, *Röntgen Centennial: X-rays in Natural and Life Sciences - Wilhelm Conrad Röntgen and the Beginning of the Modern Physics*, edited by A. Haase et al., 981-02-3085-0 (World Scientific, 1997).

[3] M. v. Laue, Bayerische Akademie der Wissenschaften - Sitzungsberichte, Sitzungsberichte (1912).

[4] W. Friedrich et al., Bayerische Akademie der Wissenschaften - Sitzungsberichte, Sitzungsberichte (1912).

[5] M. Laue, Annalen der Physik **346**, 989–1002 (1913)
DOI: 10.1002/andp.19133461005.

[6] W. H. Bragg et al., Proceedings of the Royal Society of London A: Mathematical, Physical and Engineering Sciences **88**, 428–438 (1913)
DOI: 10.1098/rspa.1913.0040.

[7] N. Bohr, Nature **92**, 231–232 (1913)
DOI: 10.1038/092231d0.

[8] H. Moseley, Philosophical Magazine Series 6 **26**, 1024–1034 (1913)
DOI: 10.1080/14786441308635052.

[9] T. Maiman, Nature **187**, 493–494 (1960)
DOI: 10.1038/187493a0.

[10] J. L. Krause et al., Phys. Rev. Lett. **68**, 3535–3538 (1992)
DOI: 10.1103/PhysRevLett.68.3535.

[11] X. F. Li et al., Phys. Rev. A **39**, 5751–5761 (1989)
DOI: 10.1103/PhysRevA.39.5751.

[12] P. B. Corkum, Phys. Rev. Lett. **71**, 1994–1997 (1993)
DOI: 10.1103/PhysRevLett.71.1994.

[13] J. Seres et al., Nature **433**, 596–596 (2005)
DOI: 10.1038/433596a.

This project has received funding from the *European Union's Horizon 2020 research and innovation programme* under grant agreement No 654220.

[14] Abraham et al., C.R. Acad. Sci. **129**, 206 (1899).

[15] R. W. Hellwarth, in To be published in advances in quantum electronics (1961).

[16] F. J. McClung et al., Journal of Applied Physics **33**, 828–829 (1962)
DOI: http://dx.doi.org/10.1063/1.1777174.

[17] A. Töpler, Annalen der Physik **207**, 180–215 (1867)
DOI: 10.1002/andp.18672070603.

[18] A. H. Zewail, The Journal of Physical Chemistry A **104**, 5660–5694 (2000)
DOI: 10.1021/jp001460h.

[19] A. J. DeMaria et al., Applied Physics Letters **8**, 174–176 (1966)
DOI: 10.1063/1.1754541.

[20] P. P. Sorokin et al., IBM Journal of Research and Development **10**, 162–163 (1966)
DOI: 10.1147/rd.102.0162.

[21] F. P. Schäfer et al., Applied Physics Letters **9**, 306–309 (1966)
DOI: 10.1063/1.1754762.

[22] C. V. Shank et al., Applied Physics Letters **24**, 373–375 (1974)
DOI: 10.1063/1.1655222.

[23] R. L. Fork et al., Applied Physics Letters **38**, 671–672 (1981)
DOI: 10.1063/1.92500.

[24] P. F. Moulton, Optics News **8**, 9–9 (1982)
DOI: 10.1364/ON.8.6.000009.

[25] P. F. Moulton, J. Opt. Soc. Am. B **3**, 125–133 (1986)
DOI: 10.1364/JOSAB.3.000125.

[26] W. H. Knox et al., Applied Physics Letters **46**, 1120–1121 (1985)
DOI: 10.1063/1.95728.

[27] R. L. Fork et al., Opt. Lett. **12**, 483–485 (1987)
DOI: 10.1364/OL.12.000483.

[28] D. E. Spence et al., Opt. Lett. **16**, 42–44 (1991)
DOI: 10.1364/OL.16.000042.

[29] R. Ell et al., Opt. Lett. **26**, 373–375 (2001)
DOI: 10.1364/OL.26.000373.

[30] A. H. Zewail, The Journal of Physical Chemistry **97**, 12427–12446 (1993)
DOI: 10.1021/j100150a001.

[31] M. Hentschel et al., Nature **414**, 509–513 (2001)
DOI: 10.1038/35107000.

This project has received funding from the *European Union's Horizon 2020 research and innovation programme* under grant agreement No 654220.

[32] E. Goulielmakis et al., Science **320**, 1614–1617 (2008)
DOI: 10.1126/science.1157846.

[33] G. Krauss et al., Nat Photon **4**, 33–36 (2010)
DOI: 10.1038/nphoton.2009.258.

[34] J. Feldhaus et al., Journal of Physics B: Atomic, Molecular and Optical Physics **38**, S799 (2005)
DOI: 10.1088/0953-4075/38/9/023.

[35] L. Gudzenko et al., Sov.Phys.Doklady **10**, 147 (1964).

[36] M. A. Duguay et al., Applied Physics Letters **10**, 350–352 (1967)
DOI: 10.1063/1.1728208.

[37] R. C. Elton, Appl. Opt. **14**, 97–101 (1975)
DOI: 10.1364/AO.14.000097.

[38] R. W. Waynant et al., Proceedings of the IEEE **64**, 1059–1092 (1976)
DOI: 10.1109/PROC.1976.10273.

[39] R. Elton, *X-ray lasers* (Academic Press, 1990).

[40] D. Attwood et al., AIP Conference Proceedings **118**, 294–313 (1984)
DOI: 10.1063/1.34644.

[41] F. E. Irons et al., Journal of Physics B: Atomic and Molecular Physics **7**, 1109 (1974)
DOI: 10.1088/0022-3700/7/9/023.

[42] J. M. J. Madey, Journal of Applied Physics **42**, 1906–1913 (1971)
DOI: 10.1063/1.1660466.

[43] D. A. G. Deacon et al., Phys. Rev. Lett. **38**, 892–894 (1977)
DOI: 10.1103/PhysRevLett.38.892.

[44] A. Kondratenko et al., Part. Accel. **10**, 207 (1980).

[45] Y. Derbenev et al., Nuclear Instruments and Methods in Physics Research **193**, 415–421 (1982)
DOI: 10.1016/0029-554X(82)90233-6.

[46] R. Bonifacio et al., Optics Communications **50**, 373–378 (1984)
DOI: 10.1016/0030-4018(84)90105-6.

[47] J. Murphy et al., Nuclear Instruments and Methods in Physics Research Section A: Accelerators, Spectrometers, Detectors and Associated Equipment **237**, 159–167 (1985)
DOI: 10.1016/0168-9002(85)90344-4.

[48] S. V. Milton et al., Science **292**, 2037–2041 (2001)
DOI: 10.1126/science.1059955.

This project has received funding from the *European Union's Horizon 2020 research and innovation programme* under grant agreement No 654220.

[49] A. Tremaine et al., Phys. Rev. Lett. **88**, 204801 (2002)
DOI: 10.1103/PhysRevLett.88.204801.

[50] V. Ayvazyan et al., Phys. Rev. Lett. **88**, 104802 (2002)
DOI: 10.1103/PhysRevLett.88.104802.

[51] V. Ayvazyan et al., English, The European Physical Journal D - Atomic, Molecular, Optical and Plasma Physics **37**, 297–303 (2006)
DOI: 10.1140/epjd/e2005-00308-1.

[52] B. W. J. McNeil et al., Nat Photon **4**, 814–821 (2010)
DOI: 10.1038/nphoton.2010.239.

[53] Z. Huang et al., Phys. Rev. ST Accel. Beams **10**, 034801 (2007)
DOI: 10.1103/PhysRevSTAB.10.034801.

[54] M. Altarelli, Nuclear Instruments and Methods in Physics Research Section B: Beam Interactions with Materials and Atoms **269**, Proceedings of the 10th European Conference on Accelerators in Applied Research and Technology (ECAART10), 2845–2849 (2011)
DOI: 10.1016/j.nimb.2011.04.034.

[55] C. Pellegrini et al., Rev. Mod. Phys. **88**, 015006 (2016)
DOI: 10.1103/RevModPhys.88.015006.

[56] *European XFEL media database*, online: https://media.xfel.eu/XFELmediabank, 2016.

[57] M. Altarelli, *The European Free-Electron Laser Facility and the Challenges of our Time*, online: http://www.xfel.eu/documents/flyers_and_brochures/, 2016.

[58] C. Bressler et al., European X-Ray Free-Electron Laser Facility GmbH (2012)
DOI: 10.3204/XFEL.EU/TR-2012-008.

[59] G. A. Mourou et al., *Eli whitebook - science and technology with ultra-intense lasers*, tech. rep. (ELI - Extreme Light Infrastructure, 2011).

[60] G. Korn et al., *Eli beamlines - summary of user requirement specifications*, tech. rep. (ELI, 2012).

[61] T. Tschentscher, *European Cluster of Advanced Laser Light Sources (EUCALL) - Proposal Part B*, tech. rep. (Horizon 2020, 2014).

[62] H. Hertz, Annalen der Physik **267**, 983–1000 (1887)
DOI: 10.1002/andp.18872670827.

[63] A. Einstein, Annalen der Physik **322**, 132–148 (1905)
DOI: 10.1002/andp.19053220607.

This project has received funding from the *European Union's Horizon 2020 research and innovation programme* under grant agreement No 654220.

[64] V. Schmidt, Reports on Progress in Physics **55**, 1483–1659 (1992)
DOI: 10.1088/0034-4885/55/9/003.

[65] W. Ackermann et al., Nat Photon **1**, 336–342 (2007)
DOI: 10.1038/nphoton.2007.76.

[66] K. Tiedtke et al., AIP Conference Proceedings **705**, 588–592 (2004)
DOI: 10.1063/1.1757865.

[67] K. Tiedtke et al., New Journal of Physics **11**, 023029 (2009)
DOI: 10.1088/1367-2630/11/2/023029.

[68] B. Faatz et al., New Journal of Physics **18**, 062002 (2016)
DOI: 10.1088/1367-2630/18/6/062002.

[69] M. Braune et al., Journal of Synchrotron Radiation **23**, 10–20 (2016)
DOI: 10.1107/S1600577515022675.

[70] E. Allaria et al., Nat Photon **6**, 699–704 (2012)
DOI: 10.1038/nphoton.2012.233.

[71] M. Zangrando et al., Review of Scientific Instruments **80**, 113110 (2009)
DOI: http://dx.doi.org/10.1063/1.3262502.

[72] J. Grünert et al., in Fel2014 (Free Electron Laser Conference 2014, Basel (Switzerland), 25 Aug 2014 - 29 Aug 2014, 2014), p. 4.

[73] J. Grünert et al., in Proceedings of the 37th international free electron laser conference (37th International Free Electron Laser Conference, Daejeon (South Korea), 23 Aug 2015 - 28 Aug 2015, Aug. 2015), WED03.

[74] P. Emma et al., Nat Photon **4**, 641–647 (2010)
DOI: 10.1038/nphoton.2010.176.

[75] K. Tiedtke et al., Journal of Applied Physics **103**, 094511, 094511 (2008)
DOI: 10.1063/1.2913328.

[76] K. Tiedtke et al., Opt. Express **22**, 21214–21226 (2014)
DOI: 10.1364/OE.22.021214.

[77] B. L. Henke et al., Atomic Data and Nuclear Data Tables **54**, 181–342 (1993)
DOI: 10.1006/adnd.1993.1013.

[78] F. Sorgenfrei et al., Review of Scientific Instruments **81**, 043107 (2010)
DOI: 10.1063/1.3374166.

[79] M. Wöstmann et al., Journal of Physics B: Atomic, Molecular and Optical Physics **46**, 164005 (2013)
DOI: 10.1088/0953-4075/46/16/164005.

This project has received funding from the *European Union's Horizon 2020 research and innovation programme* under grant agreement No 654220.

[80] A. Gottwald et al., Metrologia **43**, S125 (2006)
DOI: 10.1088/0026-1394/43/2/S25.

[81] A. Gottwald et al., Measurement Science and Technology **21**, 125101 (2010)
DOI: 10.1088/0957-0233/21/12/125101.

[82] B. Beckhoff et al., physica status solidi (b) **246**, 1415–1434 (2009)
DOI: 10.1002/pssb.200945162.

[83] T. Leitner et al., New Journal of Physics **13**, 093003 (2011)
DOI: 10.1088/1367-2630/13/9/093003.

[84] F. Rother et al., Zeitschrift für Physik **81**, 771–775 (1933)
DOI: 10.1007/BF01342072.

[85] V. Lashkaryov, Izv. Akad. Nauk SSSR, Ser. Fiz **5**, 442–446 (1941).

[86] M. Riordan et al., IEEE Spectrum **34**, 46–51 (1997)
DOI: 10.1109/6.591664.

[87] G. C. Idzorek et al., Proc. SPIE **3114**, 349–356 (1997)
DOI: 10.1117/12.278897.

[88] S. Xia et al., in Instrumentation and measurement technology conference proceedings, 2008. imtc 2008. ieee (May 2008), pp. 1956–1959,
DOI: 10.1109/IMTC.2008.4547368.

[89] V. V. Zabrodsky et al., Proc. SPIE **8777**, pages (2013)
DOI: 10.1117/12.2017478.

[90] K. Solt et al., Applied Physics Letters **69**, 3662–3664 (1996)
DOI: 10.1063/1.117016.

[91] F. Scholze et al., Proc. SPIE **4688**, 680–689 (2002)
DOI: 10.1117/12.472342.

[92] R. Korde et al., Appl. Opt. **26**, 5284–5290 (1987)
DOI: 10.1364/AO.26.005284.

[93] M. Krumrey et al., Nuclear Instruments and Methods in Physics Research Section A: Accelerators, Spectrometers, Detectors and Associated Equipment **467–468, Part 2**, Proceedings of the 7th Int. Conf. on Synchrotron Radiation Instru mentation, 1175–1178 (2001)
DOI: 10.1016/S0168-9002(01)00598-8.

[94] R. Korde et al., Metrologia **40**, S145 (2003)
DOI: 10.1088/0026-1394/40/1/333.

This project has received funding from the *European Union's Horizon 2020 research and innovation programme* under grant agreement No 654220.

[95] B. Beckhoff et al., Nuclear Instruments and Methods in Physics Research Section A: Accelerators, Spectrometers, Detectors and Associated Equipment **444**, 480–483 (2000) DOI: 10.1016/S0168-9002(99)01427-8.

[96] F. Scholze et al., Nuclear Instruments and Methods in Physics Research Section A: Accelerators, Spectrometers, Detectors and Associated Equipment **439**, 208–215 (2000) DOI: 10.1016/S0168-9002(99)00937-7.

[97] T. Tanaka et al., Nuclear Instruments and Methods in Physics Research Section A: Accelerators, Spectrometers, Detectors and Associated Equipment **659**, 528–530 (2011) DOI: 10.1016/j.nima.2011.08.039.

[98] M. Kato et al., Nuclear Instruments and Methods in Physics Research Section A: Accelerators, Spectrometers, Detectors and Associated Equipment **612**, 209–211 (2009) DOI: 10.1016/j.nima.2009.10.141.

[99] T. Tanaka et al., Review of Scientific Instruments **86**, 093104 (2015) DOI: 10.1063/1.4929666.

[100] T. Tanaka et al., Metrologia **53**, 98 (2016) DOI: 10.1088/0026-1394/53/1/98.

[101] M. Kato et al., Metrologia **47**, 518 (2010) DOI: 10.1088/0026-1394/47/5/002.

[102] N. Saito et al., Metrologia **47**, 21 (2010) DOI: 10.1088/0026-1394/47/1/003.

[103] ISO 3669, International Organization for Standardization (2015).

[104] FS-BT et al., *Technical specification - conflat flanges - vacuum applications*, tech. rep. 1.5 (Deutsches-Elektronen Synchrotron (DESY), 2011).

[105] P. J. Mohr et al., Rev. Mod. Phys. **84**, 1527–1605 (2012) DOI: 10.1103/RevModPhys.84.1527.

[106] C. Walker et al., Scanning **30**, 365–380 (2008) DOI: 10.1002/sca.20124.

[107] P. Tolias, Plasma Physics and Controlled Fusion **56**, 123002 (2014) DOI: 10.1088/0741-3335/56/12/123002.

[108] I. Bronstein et al., Moscow: Nauka (1969).

[109] Z. J. Ding et al., Journal of Applied Physics **89**, 718–726 (2001) DOI: 10.1063/1.1331645.

This project has received funding from the *European Union's Horizon 2020 research and innovation programme* under grant agreement No 654220.

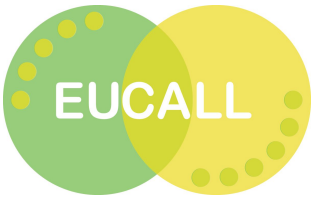

[110] J. Viefhaus et al., Nuclear Instruments and Methods in Physics Research Section A: Accelerators, Spectrometers, Detectors and Associated Equipment **710**, The 4th international workshop on Metrology for X-ray Optics, Mirror Design, and Fabrication, 151–154 (2013)
DOI: 10.1016/j.nima.2012.10.110.

This project has received funding from the *European Union's Horizon 2020 research and innovation programme* under grant agreement No 654220.